Research Article

Study on Properties of Epoxy Composites Modified by Functional Graphite Oxide and Polyurethane

Yansong Kang [1], **Zenghui Feng,**[1] **Xinhua Jiang,**[1] **Lanxuan Liu,**[1] **Jiafa Tao,**[2] **Xiwang Huang,**[1] **Weiwei Wang,**[1] **and Xiangding Xiao** [1]

[1] *Wuhan Research Institute of Materials Protection, Wuhan 430000, China*
[2] *CRRC Yangtze Co., Ltd, Wuhan 430000, China*

Correspondence should be addressed to Xiangding Xiao; 15040140333@xs.hnit.edu.cn

To improve the performance of the epoxy resin, isophorone diisocyanate (IPDI)-modified graphene oxide (GO) nanosheets were used, and the modified graphene oxide (iGO) was grafted with epoxy resin using polyurethane (PU) chain segments as a bridge to prepare epoxy composites. The iGO was characterized by Fourier transform infrared spectroscopy (FT-IR), X-ray photoelectron spectroscopy (XPS), X-ray diffraction analysis (XRD), and transmission electron microscopy (TEM), and the results showed that IPDI increased the layer spacing of iGO from 0.79 nm to 1.06 nm by grafting with hydroxyl and carboxyl groups on the surface of GO nanosheets, which improved the degree of exfoliation of iGO. Tensile testing, dynamic thermomechanical analysis (DMA), and scanning electron microscopy (SEM) were used to figure out the thermomechanical properties of the modified epoxy composites. The results show that the tensile strength and elongation at break of the as-prepared 0.5% iGO-PU/EP composites are 0.2 and 6.3 times higher than those of pure EP, respectively, and that the glass transition temperature was raised by about 2°C, with a significant increase in crosslinking.

1. Introduction

Epoxy resin (EP) is a widely used thermosetting material with low shrinkage on curing, high adhesion to the substrate surface, high mechanical strength, and excellent flame retardancy, corrosion resistance, and electrical resistance for a variety of applications. However, the disadvantages of low toughness and poor resistance to crack extension of epoxy resins [1, 2] limit their application in the fields of high impact strength and high fracture strength. For this reason, a lot of research has been done on toughening epoxy resins, some of which focused on introducing rubber phases into epoxy resins to compensate for the deficiencies of their own materials.

Polyurethane (PU) is an industrially important synthetic elastomer with excellent flexibility and elasticity, as well as high tensile strength, abrasion resistance, tear resistance, and solvent resistance. PU/EP systems have been previously reported and are commonly used in coating preparation and structural mod-

ification [3, 4] to mitigate the brittleness problems of epoxy systems. Wang and Chen [5, 6] synthesized three PUs (hydroxyl, amine, and anhydride) with different functionalized end groups to toughen bisphenol epoxy resin (DGEBA)/4,4-diaminodiphenyl sulfone (DDS) systems. Studies have shown that PU/EP with different molecular weights and contents can form homogeneous or multiphase [7, 8]. Polyurethane chains can be physically entangled and chemically bonded to the epoxy network to form grafted interpenetrating polymer network structures, forming interpenetrating polymer networks (IPN). However, the use of elastomer toughening also has unavoidable drawbacks; in general, the addition of elastomers or tougheners to polymers leads to a severe decrease in tensile strength, modulus of elasticity, and flexural strength [9]. To improve their mechanical properties, the addition of fillers and pigments to epoxy coatings is a very effective modification method [10, 11]. In the past few years, many researchers have been interested in nanomaterials when making composite materials.

Graphene oxide (GO) is a nanomaterial with an ultra-high specific surface area, a unique structure (SP2 hybridized two-dimensional single molecule film), and excellent thermal properties and is an effective choice for reinforcing polymer composites [12–14]. Reports from the past show that GO and functionalized GO nanosheets can improve the mechanical properties of epoxy coatings [15–18]. The surface of GO contains carbonyl, carboxyl, and hydroxyl groups, and the oxygen-containing groups of GO can be used for chemical modification. GO can be incorporated into polymers as covalent bonds by modification, but the large number of oxygen-containing groups leads to the incompatibility of GO with most non-polar solvents, which makes it difficult to disperse in organic polymers. Due to van der Waals forces, GO nanosheets are highly susceptible to aggregation in an epoxy resin matrix, which easily leads to thermal and mechanical degradation of the resin [19, 20]. Many researchers are now modifying the surface of GO nanosheets to solve the problem of difficult GO dispersion. Guo et al. [21] showed that GO nanosheets can be easily dispersed in organic polymers by grafting onto the surface of GO containing 2,4,6-trichloro-1,3,5-triazine (TCT) and the functionalization of GO by TCT-DETA can significantly improve the dispersibility and compatibility of GO, and the tensile and flexural strengths of GO-TCT-DETA/epoxy composites are higher than those of epoxy resin. The tensile and flexural strengths of GO-TCT-DETA/epoxy composites were increased by 40.79% and 48.56%, respectively, compared to epoxy resin. Yao et al. [22] achieved uniform dispersion of GO nanosheets in epoxy resin by chemical functionalization of GO with 4-nitrophenyl diazonium salt. When the content of modified graphene nanosheets was 0.8 wt%, the tensile strength and elongation at break of epoxy nanocomposites were increased by more than 30% and 50%, respectively. When the content of modified graphene nanosheets was 5 wt%, the thermal conductivity of the epoxy nanocomposites was increased to 0.56 W/m K, which was about 2.5 times that of pure epoxy resin.

PU was used as a second phase to toughen the epoxy resin and to disperse GO by grafting functionalized GO with PU to achieve the purpose of dispersing GO while improving the strength of the material. Based on this idea, this thesis carried out a study on the chemical grafting of GO into epoxy resins via PU. Graphene oxide was covalently modified with isophorone diisocyanate (IPDI) and reacted with polyol to form a graphene oxide-urethane (iGO-PU) prepolymer. The iGO-PU prepolymer was grafted to modify the epoxy resins, and the modified products were analyzed for their properties.

2. Experimental

2.1. Main Raw Materials.
Graphene oxide (GO) is provided by Wuhan Low Dimensional Materials Research Institute Co., Ltd.; isophorone diisocyanate (IPDI) is purchased from BASF; polytetrahydrofuran ether (PTMG1000) is purchased from Taicang Company of Sinochem; bisphenol A diglycidyl ether epoxy resin (J-51) is purchased from Shanghai Junjiang New Materials sales Co., Ltd.; and diethylene methylene diamine curing agent (MH-222) is purchased from Changsha Xinde-hang Chemical Co., Ltd. Dibutyltin dilaurate (DBTDL) was purchased from Shanghai Aladdin biochemical Technology Co., Ltd., and N,N-dimethylacetamide (DMAC) and acetone are analytically pure.

2.2. Surface Modification of GO.
Disperse 2 g GO in 200 mL DMAC, ultrasonically disperse for 2 hours, then transfer to a three-necked flask, add 18 g IPDI, add 2 drops of DBTDL, gradually heat up to 90°C in an oil bath, and stir under reflux for 20 hours under a nitrogen atmosphere. The product was suction filtered, washed with acetone, and dried in vacuo to obtain the final product, iGO.

2.3. iGO-PU Prepolymer Synthesis.
In a three-necked flask equipped with IPDI, 2 drops of DBTDL were added, and iGO of different contents was added to PTMG1000 for mechanical grinding for 2 h and added dropwise to the flask, keeping the reaction temperature below 50°C. After the addition, the temperature was raised to 80°C and the reaction was allowed to react for 2 h to obtain modified graphene oxide-polyurethane prepolymers (iGO-PU) with different content.

Continue to prepare graphene oxide/polyurethane prepolymer (GO/PU) and pure polyurethane prepolymer (PU) according to the above method.

2.4. Preparation and Application of iGO-PU/EP Composites.
Fill several three-necked flasks with 60 g of each type of prepolymer, then add 240 g of epoxy resin (J51), heat to 70°C, and thoroughly stir the reaction. The specific mix is shown in Table 1. Curing agent MH-222 (the ratio of epoxy resin content to curing agent is 3:1) was added, and curing at room temperature for 12 hours and at 80°C for 4 hours was performed to obtain composite samples. The preparation process of the composite material is shown in Figure 1, and the schematic diagram of the sample synthesis reaction is shown in Figure 2.

2.5. Testing and Characterization

2.5.1. Characterization of iGO Nanosheets.
The infrared spectra of GO and iGO were obtained using the Nexus Fourier transform infrared spectrometer (FT-IR).

The diffraction spectra of GO and iGO were obtained using the D8 advance X-ray diffractometer (XRD).

The elements and energy levels of GO and iGO were obtained using the ESCALAB 250Xi X-ray photoelectron spectrometer (XPS).

The shapes of GO and iGO were obtained using the JEM-1400 Plus 120KV transmission electron microscope (TEM).

2.5.2. Composite Characterization.
The polymer composite membrane is made of a polytetrafluoroethylene plate, and the dry film thickness is 0.5 mm ±0.05 mm. The mechanical properties of the composites were analyzed by dynamic thermomechanical analysis (DMA) and tensile test.

Using an Instron 5967 tensile testing machine, the room temperature tensile test was carried out at the strain rate of 5 mm/min.

TABLE 1: Preparation schemes for epoxy resins and different composites.

Sample	J51 (wt%)	PU (wt%)	GO (wt%)	iGO (wt%)
EP	100	0	0	0
0.5% iGO/EP	99.5	0	0	0.5
PU/EP	80	20	0	0
0.5% GO/PU/EP	80	19.5	0.5	0
0.1% iGO-PU/EP	80	19.9	0	0.1
0.5% iGO-PU/EP	80	19.5	0	0.5
1.0% iGO-PU/EP	80	19.0	0	1.0

Using a DMA Q800 dynamic thermomechanical analyzer, the storage moduli, loss factors, and glass transition temperatures of different composites were obtained at a temperature range of 25°C to 150°C, a frequency of 1 Hz, and a heating rate of 5°C/min.

The fracture morphology of the composites was obtained using the JSM-6510 scanning electron microscope (SEM).

3. Results and Discussion

3.1. Characterization of Graphene Nanosheets

3.1.1. FT-IR Analysis. The characteristic peaks of the FT-IR spectra of GO and iGO nanosheets are shown in Figure 3. The characteristic peaks of GO at $3334\,cm^{-1}$, $1731\,cm^{-1}$, $1619\,cm^{-1}$, $1234\,cm^{-1}$, and $1062\,cm^{-1}$ correspond to the stretching vibrations of O-H, C=O (carboxyl), O=C-O, C-O, and C-O-C (alkoxy), respectively. The peak of iGO near $2946\,cm^{-1}$ is attributed to a large number of C-H bonds in the alicyclic group of IPDI, and the carboxyl peak of $1731\,cm^{-1}$ almost disappears because part of IPDI reacts with carboxyl to form substituted amide derivatives. The peak at $1626\,cm^{-1}$ is amide carbonyl stretching (so-called amide I vibratory stretching). The new peaks at $1556\,cm^{-1}$ may come from amides or carbamates, corresponding to the coupling of C-N stretching vibration and N-H deformed vibration (the so-called amide II vibration) [23]. The new peaks at $3340\,cm^{-1}$ (overlapping with O-H), $750\,cm^{-1}$, and $1240\,cm^{-1}$ are related to the stretching vibration, bending vibration, and C-O stretching vibration of N-H, respectively [24]. IPDI reacts with carboxyl (-COOH) and hydroxyl (-OH) on the surface of GO to form amides and carbamates, indicating that IPDI has been successfully grafted onto the surface of GO.

3.1.2. XRD Analysis. Figure 4 shows the XRD patterns of GO and iGO nanosheets. GO shows a strong characteristic diffraction peak (001) at 11.14 [25]. The diffraction angle of iGO (001) was shifted to a lower angle ($2\theta = 8.36°$) by the surface modification of GO by IPDI. The interplanar spacing (*d*) of iGO nanoplatelets was increased from 0.79 nm to 1.06 nm. The results show that IPDI molecules are embedded between the GO sheets, resulting in an increase in the interlayer spacing of GO, and IPDI has been successfully grafted onto the edges and surfaces of GO nanosheets. In addition, compared with the sharp peaks of GO, the diffraction peak shape of iGO is obviously broadened and the diffraction intensity is reduced, which indicates that the successful grafting of IPDI destroys the original structure of the grains, makes the crystals more disordered, and further increases the distance between the lamellae, reducing the possibility of reunion.

3.1.3. XPS Analysis. The elemental composition of GO and iGO is analyzed by XPS. Figures 5(a) and 5(b) are XPS full spectra of GO and iGO, respectively. In the full spectrum of GO, ~284.1 eV and ~533.1 eV correspond to the characteristic peaks of C1s and O1s, respectively. The XPS spectrum of iGO increases the characteristic peak of N1s (~399.1 eV), which shows that the sample contains N elements. Table 2 shows the contents of carbon, oxygen, and nitrogen. It can be seen that after IPDI modification of GO, the oxygen atom content of iGO decreased from 33.67% to 17.19%, while the N atom content increased to 7.55%, indicating the introduction of N-containing groups after modification. These results show that there is a chemical reaction between GO and IPDI.

The C1s peaks of GO and iGO are shown in Figures 5(c) and 5(d). The C1s spectrum of GO is mainly composed of C=C (284.3 eV), C-C (284.8 eV), C-O (286.5 eV), C=O (carbonyl 287.0 eV), and O-C=O (carboxyl 288.5 eV). After modification, although there are the same oxygen-containing groups in the C1s of iGO, the intensity of the C-O peak becomes weaker. In addition, the C-N peak in ~286.1 eV coincides with the C-O peak to form a wide peak [26, 27], which is lower than the single peak of 0.4 eV of C-O in GO, which further indicates that some oxygen-containing groups in GO react with IPDI and form other chemical bonds. The intensity of O-C=O (288.2 eV) and C=O (287.0 eV) in the C1s peak of iGO is still very strong, which is due to the formation of NH-COO- and -NH-C=O groups. The peak intensity of the C1s spectrum of GO at a lower binding energy (~284.7 eV) is larger than that at a higher binding energy (~286.8 eV), while the opposite is true for iGO, which indicates the SP2 structure of some C atoms in iGO is destroyed to form SP3 hybrids. This shifts the GO further towards "disordering," increasing the distance between the sheets and reducing the likelihood of agglomeration. This corroborates with the results mentioned in XRD.

Figures 5(e) and 5(f) show the O1s scanning spectra of GO and iGO, respectively, and 532.6 eV and 531.0 eV are the peaks of C-O and C=O, respectively. Similar to the results of the C1s spectrum, the atomic percentage of O in the form of C=O increased from 0.03% to 27.5% due to the modification of iGO. On the one hand, it is because of the presence of unreacted -NCO groups, and on the other hand, the carboxyl groups on the graphene oxide nanosheets are consumed.

The high-resolution N1s spectrum of (g) iGO in Figure 5 shows two peaks at 399.4 eV and 400.1 eV, corresponding to -CONH and -NCO [28, 29], respectively, indicating the formation of a covalent bond between GO and IPDI.

3.1.4. TEM Analysis. The flake morphologies of GO and iGO were observed by transmission electron microscopy (TEM). It was found that the two kinds of particles had flat flake structures and no obvious agglomeration (Figure 6). In the
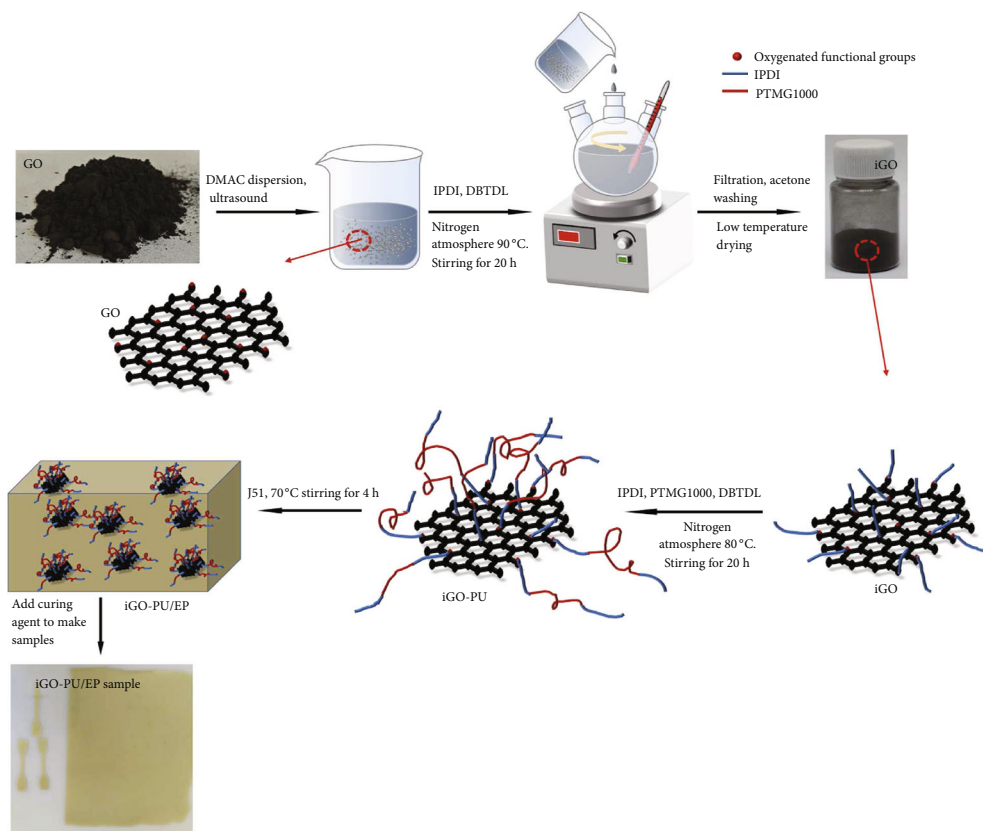
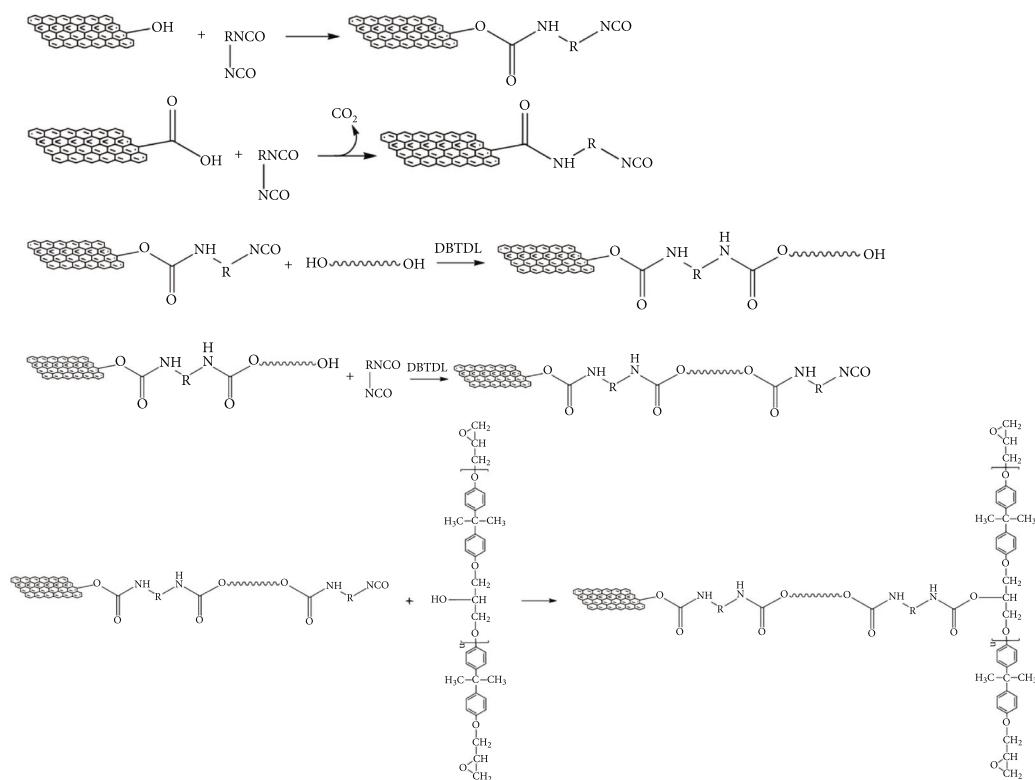FIGURE 1: Schematic diagram of sample preparation.

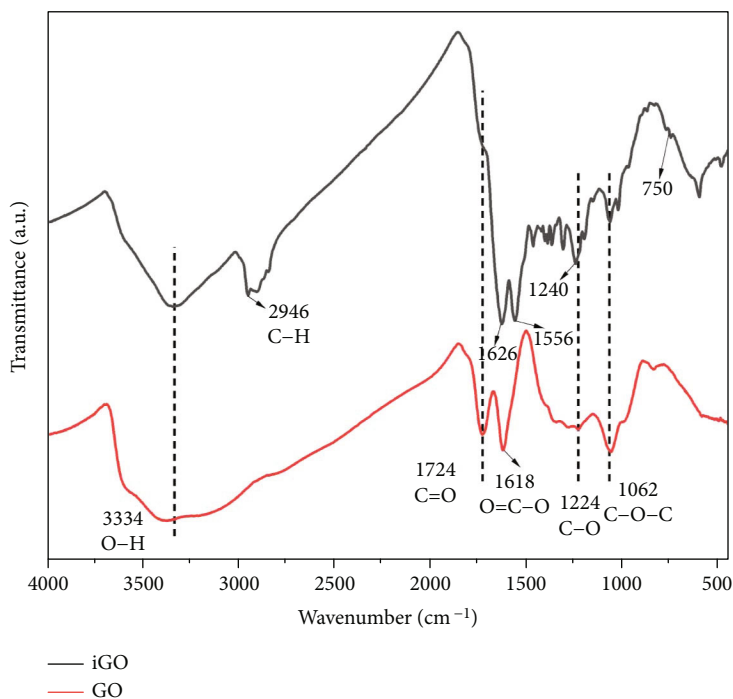FIGURE 2: Schematic diagram of the sample synthesis reaction.
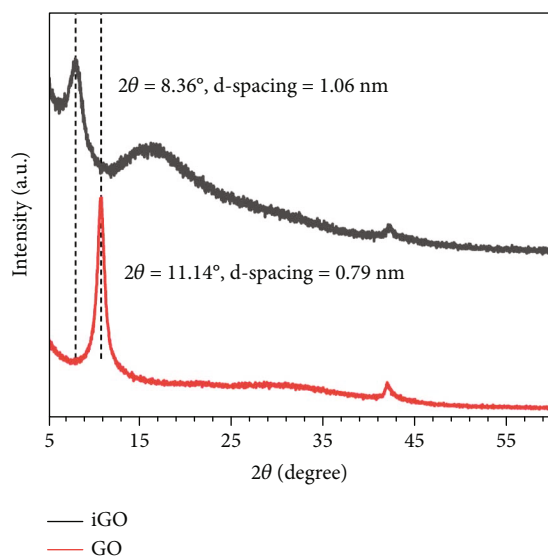
Figure 3: Infrared spectra of GO and iGO.

Figure 4: XRD patterns of GO and iGO.

process of modification, the morphology of GO changed clearly, and some worm-like particles appeared on its surface (Figure 6(b)), which was due to the grafting of IPDI onto the surface of GO. The iGO nanosheets show small size and many folds. It can be seen that part of IPDI is grafted between iGO layers, which increases the distance between layers and improves the dispersion of iGO in polar organic solvents [30].

3.1.5. iGO Dispersion and Stability Analysis. Figure 7 depicts the dispersion of iGO and GO in DMAC at 25°C. The left picture shows the sample of 0.1giGO (a) and GO (b) after ultrasonic dispersion for 30 min in 10 ml DMAC, and the picture on the right shows the sample after standing for 40 min. There was no obvious change in iGO after standing for 40 min, but GO had already settled. The dispersion stability of iGO in organic solvents was significantly improved. This is attributed to the functionalization of the hydroxyl groups on the iGO surface after modification, which reduces the density of hydrogen bond donor groups. The effect of van der Waals forces is weakened due to the increase in the interlayer spacing, and the organic solvent can pass through the layers of the GO sheet and break these hydrogen bonds [31].

Figure 8 shows the dispersion of the iGO-PU and GO/PU prepolymers at 25°C. The left picture shows the dispersion of 0.5% iGO-PU (a) and 0.5% GO/PU (b) at the beginning of the experiment, and the right picture shows the dispersion after standing for 10 days. It can be seen that after standing for 10 days, the iGO-PU hardly settles. This is attributed to the increased spacing after iGO nanosheets, which makes it easier to disperse, and after grafting -NCO groups, iGO will react with PTMG1000 containing -OH groups, increasing the steric hindrance, making it not difficult settle in the matrix. This shows good stability in PU prepolymer.

3.2. Composite Characterization

3.2.1. DMA Analysis. The DMA analysis results are shown in Figures 9(a)–9(d), including the temperature change from 30°C to 160°C, storage modulus ($E0$), and dissipation factor (tanδ). Table 3 presents the DMA data for neat epoxy and other composites. It can be seen that the storage modulus of PU/EP, 0.5%GO/PU/EP, and 0.5%iGO-PU/EP is lower than that of pure epoxy resin at 30°C because PU contains long-chain macromolecular ether bonds, reducing the strength of
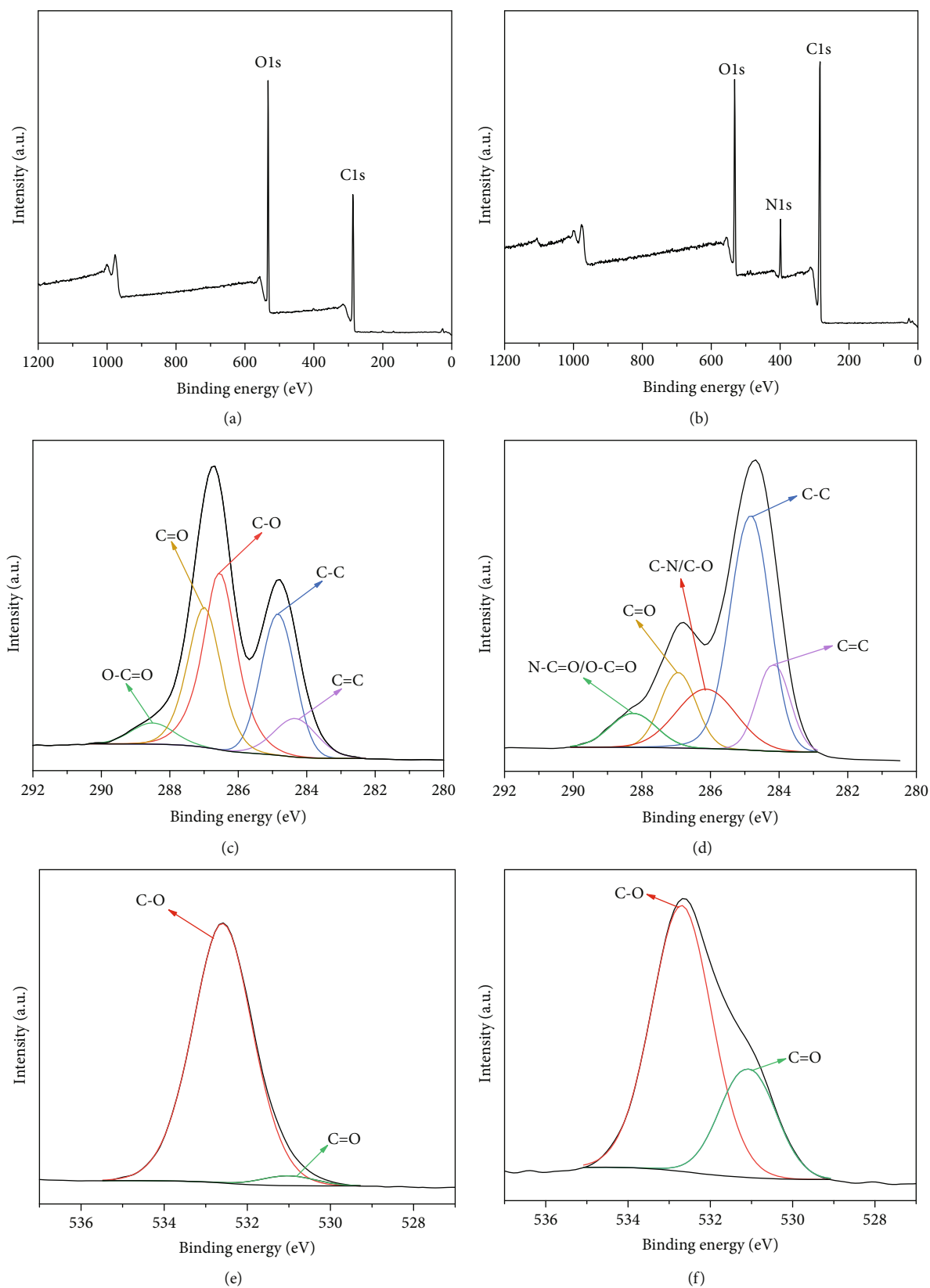
(a)

(b)

(c)
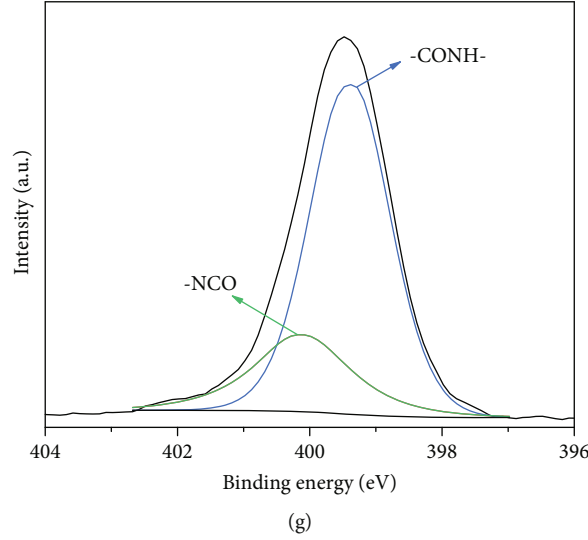
(d)

(e)

(f)

Figure 5: Continued.

(g)

FIGURE 5: (a) XPS spectrum of GO, (b) XPS spectrum of iGO, (c) C1s high-resolution spectrum of GO, (d) C1s high-resolution spectrum of iGO, (e) O1s high-resolution spectrum of GO, (f) O1s high-resolution spectrum of iGO, and (g) N1s high-resolution spectrum of iGO.

TABLE 2: XPS atomic percentage of carbon, oxygen, and nitrogen.

Sample	C (at%)	O(at%)	N (at%)
GO	66.33	33.67	0
iGO	68.28	17.19	7.55

the composite material. By adding iGO, the storage modulus of PU/EP was increased by 65%. The good dispersion of iGO in the PU and the interaction with the PU interface limit the segment motion around the iGO sheet in the PU to a certain extent. The storage modulus of the GO-added composite material is slightly higher than that of PU/EP, and the GO nanosheets can strengthen the composite material to a certain extent. There is limited improvement in the mechanical properties of composites [32].

The T_g value is the maximum peak value of the tanδ and temperature curve. T_g measures the crosslinking degree and heat resistance of epoxy composites, and the storage modulus above T_g can also reflect the crosslinking degree of epoxy composites. The higher the storage modulus, the greater the crosslinking degree. The crosslink density v is calculated by [33, 34]:

$$v = \frac{E_r}{3RT_r} \qquad (1)$$

where T_r is the temperature above T_g, E_r is the storage modulus corresponding to Tr obtained from the DMA data, and R is the actual gas constant. The obtained results are listed in Table 3.

The T_g of pure EP was 71.05°C. The T_g of EP decreased slightly with the addition of iGO, and the crosslink density reached its maximum, while the addition of PU caused the T_g to decrease by about 10°C and the crosslink density to also decrease significantly. The addition of 0.5% GO to PU/EP increased T_g by about 2°C, while the addition of 0.5% iGO

increased the T_g of PU/EP by about 11°C, and even the crosslink density and T_g values exceeded those of pure EP. This further indicates that the addition of iGO induces an increase in the crosslinking density, which is due to the sufficient crosslinking of the iGO nanosheets with the epoxy resin through the PU linker chain and the restricted movement of the epoxy resin segment and the PU macromolecular chain, which delays the glass transformation.

By adding different amounts of iGO to PU/EP, it can be found that when the amount of iGO is less than 0.5%wt, with the increase of iGO content, E0, T_g, and crosslinking density all increase. However, when 1.0%wt iGO was added, the E0, T_g, and crosslinking density decreased. This may be due to the fact that the excess iGO could not be completely grafted to PU during the preparation process, and the "free" iGO will form a large number of defects in the matrix. In addition, a large amount of iGO dispersed in the material may coat the curing agent and affect the crosslinking and curing of the material, thereby affecting the thermodynamic properties of the material [32].

3.2.2. Tensile Test Analysis. Tensile tests were performed to investigate the mechanical properties of the composites. Figure 10(a) shows the tensile curves of different types of composites, and the specific values are listed in Table 4.

It can be seen that the elongation at break of pure epoxy resin is the lowest, and the tensile strength and elongation at break of iGO-EP are improved to a certain extent. Adding iGO will improve the strength of epoxy resin to a certain extent.

After PU is added to EP, an obvious yield point appears, and the elongation at break increases from 3.25% to 10.37%, which means that the epoxy resin changes from brittleness to toughness, and the isocyanate-terminated PU can cross the hydroxyl group of the oxygen resin. The movement of the soft segment (long-chain macromolecular alcohol) in PU can greatly improve the elongation at break of epoxy resin. Generally speaking, the tensile strength, elastic modulus, and
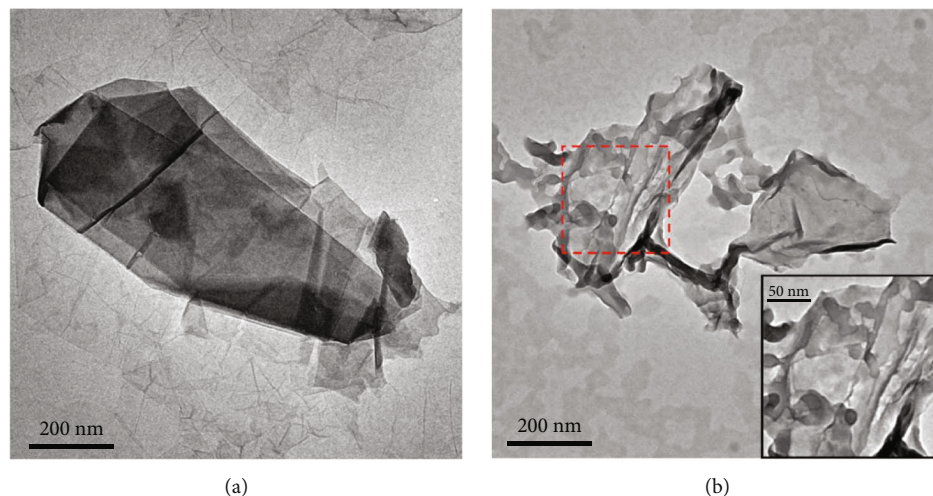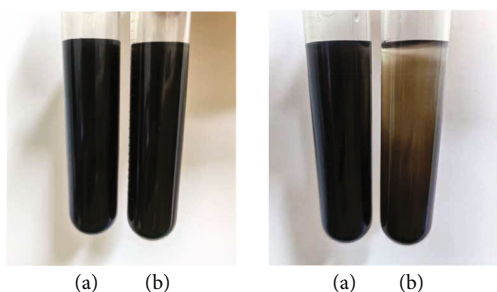
(a)

(b)

FIGURE 6: TEM images of (a) GO and (b) iGO.

(a)   (b)   (a)   (b)

FIGURE 7: Dispersion of iGO and GO in DMAC.

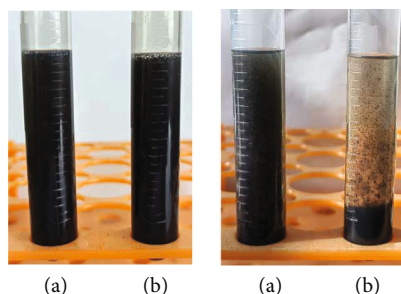(a)   (b)   (a)   (b)

FIGURE 8: Dispersion of iGO-PU and GO/PU prepolymers.

flexural strength of the material will be significantly reduced by adding elastomers or toughening agents to the polymer [9].

The tensile strength of 0.5% iGO-PU/EP composites was 48.46 MPa, and the elongation at break was 20.57%, which were significantly higher than the other samples. Compared with the pure EP composites, the tensile strength and elongation at break were 0.2 and 6.3 times higher, respectively, with significantly improved mechanical properties. This was attributed to the enhanced dispersion of iGO nanosheets in the epoxy matrix composites through PU grafting, which increased the contact area between the nanosheets and the polymer base, thus improving the transfer of stress from the epoxy matrix composites to the iGO nanosheets [35] and increasing the toughness of the material.

The tensile strength of 0.5% GO/PU/EP composites was improved compared with PU/EP, and the elongation at break was only 12.92%, which was close to that of PU/EP. The addition of GO did not further improve the elongation at break of the material, which was due to the poor dispersion of GO in the system, and the stress suffered was not uniformly dispersed, which led to the crack extension.

Next, the effect of iGO content on the composites was investigated. Figure 10(b) shows the tensile curves of iGO-PU/EP composites with different contents. It can be seen that at iGO content less than 0.5 wt%, the tensile strength and elongation at break gradually increase with increasing iGO content, and the mechanical properties of the material are improved. This changed when the iGO content was increased to 1.0 wt%, and the elongation at break decreased and was close to that of PU/EP composites without iGO addition, while the tensile strength increased and the yield point shifted to the left. It indicates that the high filling amount of iGO increases the number of defects and dislocations inside the composites and improves the stiffness of the material, which tends to lead to stress concentration and a large number of microcracks, and reduces the elongation at break of the material [36].

3.2.3. SEM Analysis. The pure EP fracture has a relatively smooth, oriented fracture pattern surface (Figure 11(a)), implying that crack propagation is unhindered. These characteristics are typical of brittle thermoset polymers [37].

The fracture surface of PU/EP composites should be relatively rough, resembling a channel-like structure and producing some microcracks with a rough and irregular fracture surface [38], implying that crack propagation requires a relatively high fracture energy.

The fracture of the 0.5% GP/PU/EP composites revealed a structural trend of crack deflection (Figure 11(c)), as well as many fine particles in the fracture, which may be related to graphene agglomeration, and agglomerated non-reticulated GO nanosheets are more likely to lead to crack sprouting and extension, reducing the toughening effect on the composites [39].
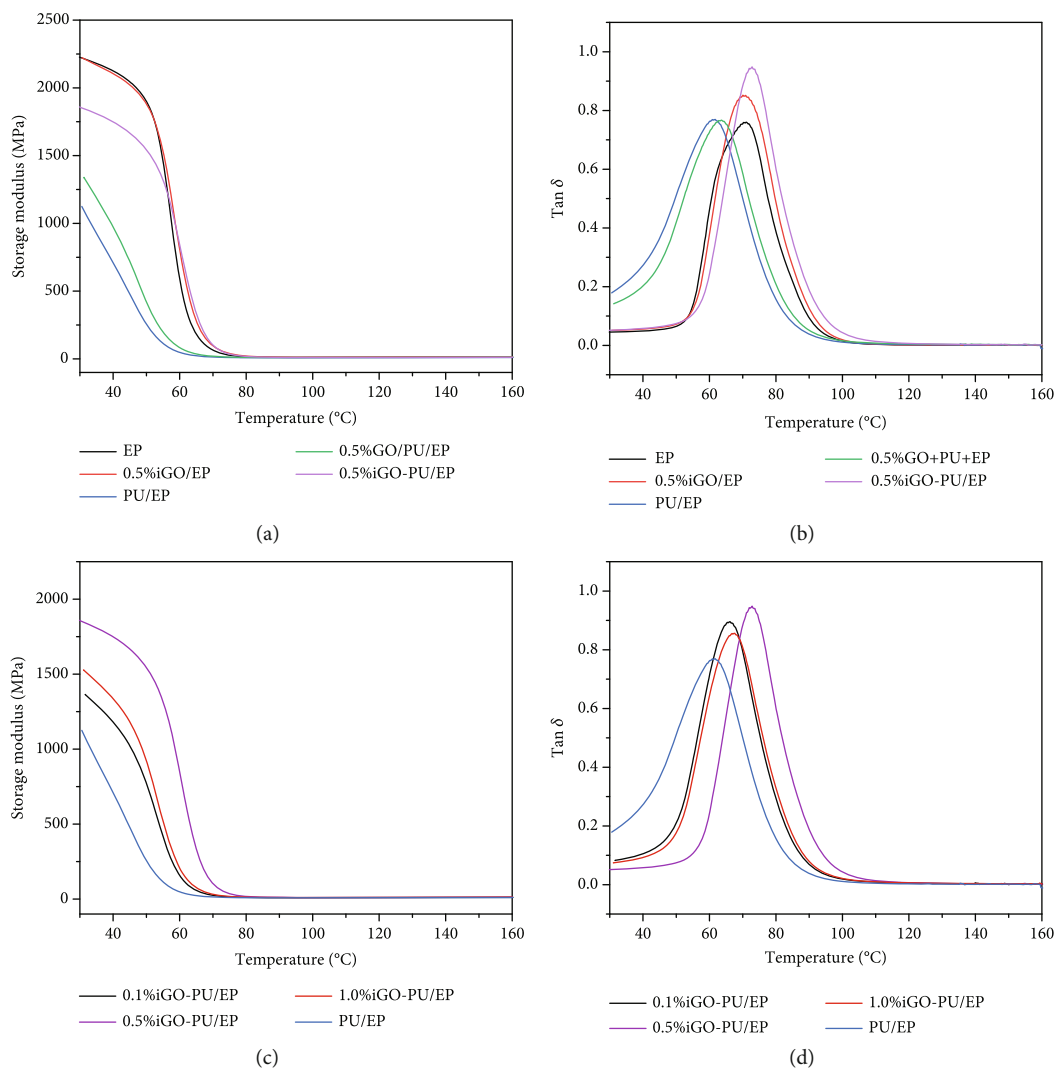
(a)

(b)

(c)

(d)

FIGURE 9: The curves of storage modulus (a) and tanδ with temperature (b) for pure epoxy resin and different composites, and the curves of storage modulus (c) and tanδ with temperature (d) for composites with different iGO contents.

TABLE 3: Storage modulus, glass transition temperature, and crosslink density of pure epoxy resin and different composites.

Sample	Storage modulus $E0$ (30˚C, MPa)	Glass transition temperature T_g (˚C)	Crosslinking density ν (mol/m^3)
EP	2212	71.05	3749.33
0.5%iGO/EP	2217	70.91	5399.27
PU/EP	1125	61.48	1236.29
0.5%GO/PU/EP	1339	63.59	1663.80
0.1%iGO-PU/EP	1364	66.23	1871.86
0.5%iGO-PU/EP	1857	72.82	5015.67
1.0%iGO-PU/EP	1528	67.6	2199.92

The fractures of 0.5% iGO-PU/EP composites show a high number of crack deflections in the form of grooves and vortex-like structures (Figure 11(d)), indicating that a greater degree of matrix deformation occurs, consuming a large amount of fracture energy and resulting in a more pronounced toughness enhancement [40]. The 0.5% iGO-PU/EP composites show much higher toughness than other materials, similar to the movement of dislocations through the crystals. Cracks in the material also have linear tension, and crack extension is hindered when encountering iGO nanosheets. Continuing to increase the stress, the cracks will bend around, resulting in an increase in fracture energy. In addition, since rigid particles do not produce large deformation, interfacial debonding between the matrix and rigid particles occurs under tensile stress, forming cavities, while the presence of greater compressive stress in rigid particles leads to premature yielding in
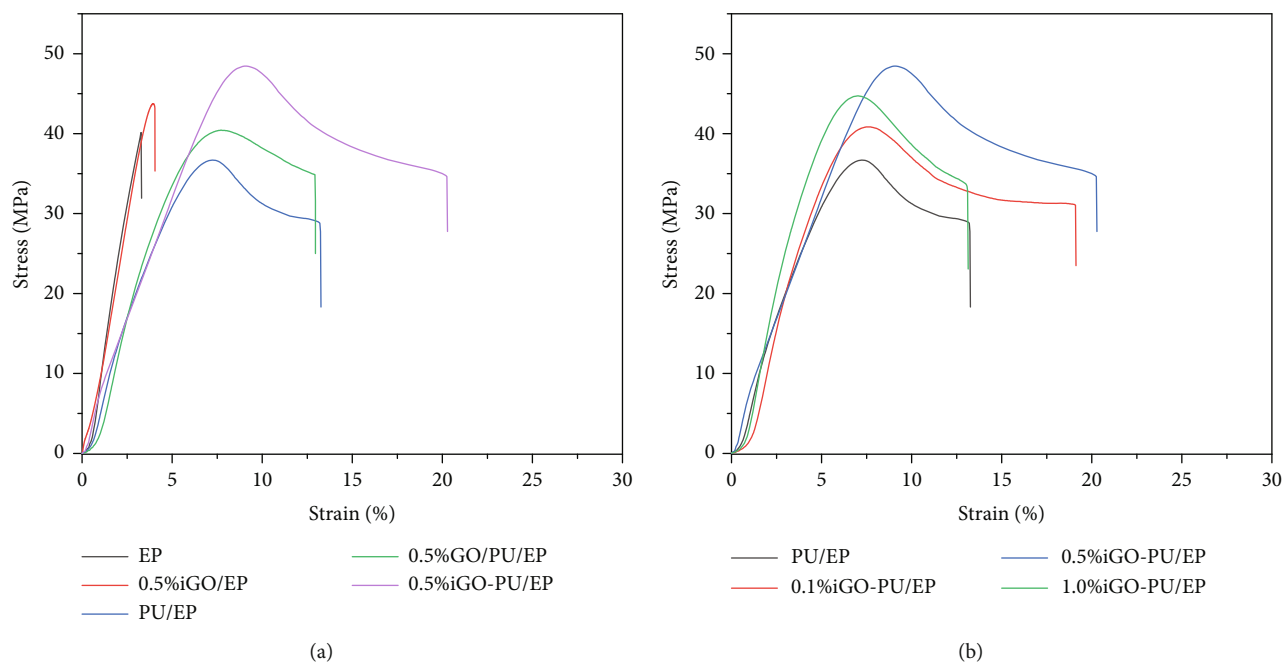
(a)

(b)

FIGURE 10: Tensile curves of different types of composites (a) and composites with different iGO contents (b).

TABLE 4: Elongation at break, tensile strength, and fracture energy of pure epoxy resin and different composites.

Sample	Elongation at break (%)	Tensile strength (MPa)	Fracture energy (J/m^2)
EP	3.28	40.13	61.51
0.5%iGO/EP	4.04	43.70	91.84
PU/EP	13.20	36.70	348.12
0.5% GO/PU/EP	12.93	40.41	381.32
0.1% iGO-PU/EP	19.10	40.84	566.72
0.5% iGO-PU/EP	20.57	48.46	701.07
1.0% iGO-PU/EP	13.10	44.69	419.28
iGO- PU/EP	26.51	40.18	247.77

(a) EP

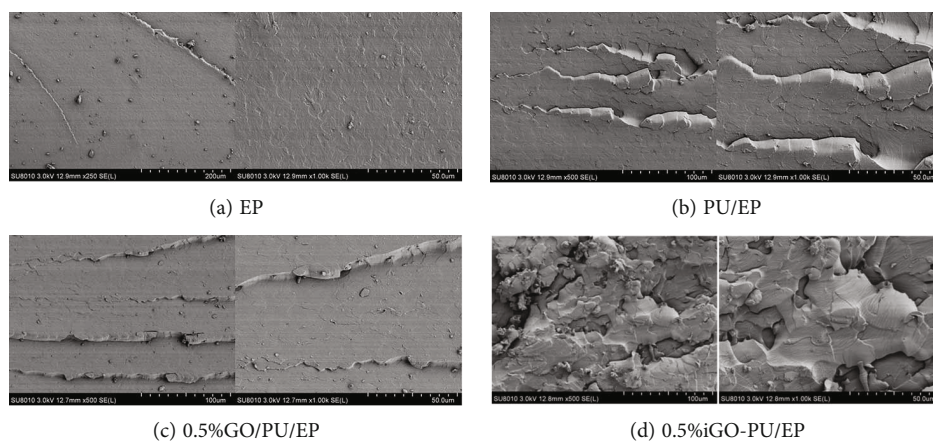(b) PU/EP

(c) 0.5%GO/PU/EP

(d) 0.5%iGO-PU/EP

FIGURE 11: Fracture topography of pure epoxy resin and different composites.

localized regions. Concentrated stresses produce yielding and interfacial debonding, both of which require more energy consumption to achieve the purpose of strengthening and toughening [41].

4. Conclusions

In this work, functionalized graphene oxide (iGO) was prepared by modifying GO nanosheets with IPDI and grafting iGO with polyurethane PU. The results showed that the layer spacing of iGO increased from 0.79 nm to 1.06 nm, and the functionalized modification significantly improved the dispersion of GO in organic solvents, which could be stably dispersed in the prepolymer for more than 10 days. The synthesized iGO-PU prepolymer was then added to epoxy resin (EP) to produce iGO-PU/EP high-tough composites. This structure of rigid lamellae grafted with flexible chain segments can improve the strength while increasing the flexibility of the epoxy resin. The results showed that the tensile strength and elongation at break of 0.5% iGO-PU/EP composites were 0.2 and 6.3 times higher than those of pure EP, respectively, and the glass transition temperature was also increased by about 2°C. This was due to the good dispersion uniformity of iGO and the high crosslinking density, which increases the contact area between the nanosheets and the polymer matrix, improves the stress transfer from the epoxy-based composite to the iGO nanosheets, and increases the toughness of the material.

In this paper, the synthesis and grafting of iGO provide a new idea to prevent the agglomeration of nano-fillers in polymers, while the toughening of epoxy resin by grafting graphene oxide with elastomer overcomes some drawbacks (significant decrease in heat resistance and strength) of pure elastomer toughening. It has been shown that iGO-PU/EP composites could be used in special fields that need high toughness and high impact strength.

Data Availability

All data and information recorded or analyzed throughout this study are included in this paper.

Conflicts of Interest

The authors declare that they have no conflicts of interest.

References

[1] B. Wetzel, P. Rosso, F. Haupert, and K. J. E. Friedrich, "Epoxy nanocomposites-fracture and toughening mechanisms," *Engineering fracture mechanics*, vol. 73, no. 16, pp. 2375–2398, 2006.

[2] P. Rosso and L. J. M. Ye, "Epoxy/silica nanocomposites: nanoparticle-induced cure kinetics and microstructure," *Macromolecular rapid communications*, vol. 28, no. 1, pp. 121–126, 2007.

[3] C. B. Qu, T. Wu, G. W. Huang et al., "Improving cryogenic mechanical properties of carbon fiber reinforced composites based on epoxy resin toughened by hydroxyl-terminated poly-

[4] T. Wu, Y. Liu, N. Li, G. W. Huang, C. B. Qu, and H. M. Xiao, "Cryogenic mechanical properties of epoxy resin toughened by hydroxyl- terminated polyurethane," *Polymer Testing*, vol. 74, pp. 45–56, 2019.

[5] H. H. Wang and J. C. Chen, "Modification and compatibility of epoxy resin with hydroxyl-terminated or amine-terminated polyurethanes," *Polymer Engineering & Science*, vol. 35, no. 18, pp. 1468–1475, 1995.

[6] H. H. Wang and J. C. Chen, "Toughening of epoxy resin by functional-terminated polyurethanes and/or semicrystalline polymer powders," *Journal of applied polymer science*, vol. 82, no. 12, pp. 2903–2912, 2001.

[7] Y. C. Chern, K. H. Hsieh, and J. S. Hsu, "Interpenetrating polymer networks of polyurethane cross-linked epoxy and polyurethanes," *Journal of materials science*, vol. 32, no. 13, pp. 3503–3509, 1997.

[8] D. S. Kim, K. Cho, J. H. An, and C. E. Park, "Toughening mechanisms of modified unsaturated polyester with novel liquid polyurethane rubber," *Journal of materials science*, vol. 29, no. 7, pp. 1854–1866, 1994.

[9] H. N. Tien, N. T. Hien, E. S. Oh et al., "Synthesis of a highly conductive and large surface area graphene oxide hydrogel and its use in a supercapacitor," *Journal of Materials Chemistry A*, vol. 1, no. 2, pp. 208–211, 2013.

[10] B. Ramezanzadeh, A. Ahmadi, and M. J. C. S. Mahdavian, "Enhancement of the corrosion protection performance and cathodic delamination resistance of epoxy coating through treatment of steel substrate by a novel nanometric sol-gel based silane composite film filled with functionalized graphene oxide nanosheets," *Corrosion Science*, vol. 109, pp. 182–205, 2016.

[11] A. Javidparvar, B. Ramezanzadeh, and E. J. P. Ghasemi, "Effects of surface morphology and treatment of iron oxide nanoparticles on the mechanical properties of an epoxy coating," *Progress in organic coatings*, vol. 90, pp. 10–20, 2016.

[12] J. Shen, M. Shi, H. Ma et al., "Synthesis of hydrophilic and organophilic chemically modified graphene oxide sheets," *Journal of colloid and interface science*, vol. 352, no. 2, pp. 366–370, 2010.

[13] Z. Li, R. J. Young, R. Wang et al., "The role of functional groups on graphene oxide in epoxy nanocomposites," *Polymer*, vol. 54, no. 21, pp. 5821–5829, 2013.

[14] L. Lei, J. Shan, J. Hu, X. Liu, J. Zhao, and Z. J. C. S. Tong, "Co-curing effect of imidazole grafting graphene oxide synthesized by one-pot method to reinforce epoxy nanocomposites," *Composites Science and Technology*, vol. 128, pp. 161–168, 2016.

[15] N. D. Alexopoulos, Z. Paragkamian, P. Poulin, and S. K. Kourkoulis, "Fracture related mechanical properties of low and high graphene reinforcement of epoxy nanocomposites," *Composites Science and Technology*, vol. 150, pp. 194–204, 2017.

[16] P. Gogoi, R. Boruah, and S. K. Dolui, "Jatropha curcas oil based alkyd/epoxy/graphene oxide (GO) bionanocomposites: Effect of GO on curing, mechanical and thermal properties," *Progress in Organic Coatings*, vol. 84, pp. 128–135, 2015.

[17] P. A. Okafor, J. Singh-Beemat, and J. O. Iroh, "Thermomechanical and corrosion inhibition properties of graphene/epoxy ester- siloxane-urea hybrid polymer nanocomposites," *Progress in Organic Coatings*, vol. 88, pp. 237–244, 2015.

[18] A. K. Pathak, M. Borah, A. Gupta, T. Yokozeki, and S. R. Dhakate, "Improved mechanical properties of carbon fiber/

graphene oxide-epoxy hybrid composites," *Composites Science and Technology*, vol. 135, pp. 28–38, 2016.

[19] B. Shen, W. Zhai, M. Tao, D. Lu, and W. Zheng, "Chemical functionalization of graphene oxide toward the tailoring of the interface in polymer composites," *Composites Science and Technology*, vol. 77, pp. 87–94, 2013.

[20] S. Y. Lee, M. H. Chong, M. Park, H. Y. Kim, and S. J. Park, "Effect of chemically reduced graphene oxide on epoxy nanocomposites for flexural behaviors," *Carbon letters*, vol. 15, no. 1, pp. 67–70, 2014.

[21] S. Guo, L. Ma, G. Song et al., "Covalent grafting of triazine derivatives onto graphene oxide for preparation of epoxy composites with improved interfacial and mechanical properties," *Journal of Materials Science*, vol. 53, no. 24, pp. 16318–16330, 2018.

[22] H. Yao, S. A. Hawkins, and H. J. Sue, "Preparation of epoxy nanocomposites containing well-dispersed graphene nanosheets," *Composites Science and Technology*, vol. 146, pp. 161–168, 2017.

[23] H. Günzler and H.-U. Gremlich, *IR-Spektroskopie: Eine Einführung*, John Wiley & Sons, 2012.

[24] B. Di Credico, M. Levi, and S. Turri, "An efficient method for the output of new self-repairing materials through a reactive isocyanate encapsulation," *European Polymer Journal*, vol. 49, no. 9, pp. 2467–2476, 2013.

[25] P. Song, Z. Cao, Y. Cai, L. Zhao, Z. Fang, and S. Fu, "Fabrication of exfoliated graphene-based polypropylene nanocomposites with enhanced mechanical and thermal properties," *Polymer*, vol. 52, no. 18, pp. 4001–4010, 2011.

[26] P. Lin, L. Meng, Y. Huang, L. Liu, and D. Fan, "Simultaneously functionalization and reduction of graphene oxide containing isocyanate groups," *Applied Surface Science*, vol. 324, pp. 784–790, 2015.

[27] J.-J. Bai, G.-S. Hu, J.-T. Zhang et al., "Preparation and rheology of isocyanate functionalized graphene oxide/thermoplastic polyurethane elastomer nanocomposites," *Journal of Macromolecular Science, Part B*, vol. 58, no. 3, pp. 425–441, 2019.

[28] Y. Xue, J. Liu, H. Chen et al., "Nitrogen-doped graphene foams as metal-free counter electrodes in high-performance dye-sensitized solar cells," *Angewandte Chemie International Edition*, vol. 51, no. 48, pp. 12124–12127, 2012.

[29] J. Che, Y. Xiao, X. Wang, A. Pan, W. Yuan, and X. Wu, "Grafting polymerization of polyacetal onto nano-silica surface via bridging isocyanate," *Surface and Coatings Technology*, vol. 201, no. 8, pp. 4578–4584, 2007.

[30] J. Shen, M. Zhang, G. Liu, K. Guan, and W. Jin, "Size effects of graphene oxide on mixed matrix membranes for CO2 separation," *AICHE Journal*, vol. 62, no. 8, pp. 2843–2852, 2016.

[31] S. Stankovich, R. D. Piner, S. T. Nguyen, and R. S. Ruoff, "Synthesis and exfoliation of isocyanate-treated graphene oxide nanoplatelets," *Carbon*, vol. 44, no. 15, pp. 3342–3347, 2006.

[32] S. Chhetri, P. Samanta, N. C. Murmu, S. K. Srivastava, and T. Kuila, "Effect of dodecyal amine functionalized graphene on the mechanical and thermal properties of epoxy-based composites," *Polymer Engineering & Science*, vol. 56, no. 11, pp. 1221–1228, 2016.

[33] M. Lotfi, A. Azizi, H. Yari, and M. Ganjaee Sari, "Aminosilane-co-graphene oxide/epoxy nanocomposite coating: an approach towards toughness and viscoelastic properties enhancement," *Progress in Organic Coatings*, vol. 151, p. 106050, 2021.

[34] J. S. Jayan, A. Saritha, B. D. S. Deeraj, and K. Joseph, "Triblock copolymer grafted graphene oxide as nanofiller for toughening of epoxy resin," *Materials Chemistry and Physics*, vol. 248, p. 122930, 2020.

[35] X. Wang, W. Xing, P. Zhang, L. Song, H. Yang, and Y. Hu, "Covalent functionalization of graphene with organosilane and its use as a reinforcement in epoxy composites," *Composites science and technology*, vol. 72, no. 6, pp. 737–743, 2012.

[36] M. Sahu and A. M. Raichur, "Toughening of high performance tetrafunctional epoxy with poly(allyl amine) grafted graphene oxide," *Composites Part B: Engineering*, vol. 168, pp. 15–24, 2019.

[37] H. Kulkarni, P. Tambe, and G. Joshi, "High concentration exfoliation of graphene in ethyl alcohol using block copolymer surfactant and its influence on properties of epoxy nanocomposites," *Fullerenes, Nanotubes and Carbon Nanostructures*, vol. 25, no. 4, pp. 241–249, 2017.

[38] L. Pan, J. Ban, S. Lu et al., "Improving thermal and mechanical properties of epoxy composites by using functionalized graphene," *RSC Advances*, vol. 5, no. 74, pp. 60596–60607, 2015.

[39] B. Qi, Z. Yuan, S. Lu et al., "Mechanical and thermal properties of epoxy composites containing graphene oxide and liquid crystalline epoxy," *Fibers and Polymers*, vol. 15, no. 2, pp. 326–333, 2014.

[40] M. Naeem, H. C. Kuan, A. Michelmore et al., "A new method for preparation of functionalized graphene and its epoxy nanocomposites," *Composites Part B: Engineering*, vol. 196, article 108096, 2020.

[41] M. Rubinstein and R. H. Colby, *Polymer physics*, vol. 23, Oxford university press, New York, 2003.